Available online at www.sciencedirect.com
ScienceDirect
Catalysis Today 119 (2007) 204–208
CATALYSIS TODAY
www.elsevier.com/locate/cattod

The physicochemical properties of rutile-supported V-O-Mo catalyst

P. Kornelak [a,*], B. Borzęcka-Prokop [a], L. Lityńska-Dobrzyńska [b], J. Wagner [c], D.S. Su [c], J. Camra [d], A. Wesełucha-Birczyńska [d]

[a] *Faculty of Chemistry, Jagiellonian University, Ingardena 3, 30 060 Krakow, Poland*
[b] *Institute of Metallurgy and Materials Science, PAS, Reymonta 25, Krakow, Poland*
[c] *Department of Inorganic Chemistry, Fritz-Haber-Institut der Max-Planck Geselleschaft, Faradayweg 4-6, D-14195 Berlin, Germany*
[d] *Regional Laboratory of Physicochemical Analyses and Structural Research, Jagiellonian University, Ingardena 3, 30 060 Krakow, Poland*

Available online 11 September 2006

Abstract

This paper concerns the physicochemical properties and activity in NO decomposition of a rutile-supported V-O-Mo catalyst, obtained by sol–gel method. Rutile, o-MoO_3 and β-MoO_3 are the main phases found by XRD and TEM. Monolayer vanadia-like species containing some Mo atoms substituted for V ones are present on molybdena crystallites. These species show some activity in NO decomposition to N_2 and O_2. An increase in this activity with the increase of O_2 content in the feed indicates surface reconstruction occurring due to interaction with oxygen.

Keywords: Rutile-supported V-O-Mo catalyst; Sol–gel method; XRD; TEM; FT Raman Spectroscopy

1. Introduction

V-O-Mo catalysts are used for selective catalytic reduction of NO by NH_3 when arsenic is present in effluent gases. They show also some activity in direct NO decomposition to N_2 and O_2 [1,2]. Vanadia surface species were revealed to be responsible for both processes. Anatase is usually used as a support for that catalyst. Being a metastable TiO_2 polymorph, the drawback of anatase is its gradual transformation into stable rutile [3]. The temperature of transformation, equal to ca. 1100 K for crystalline pure anatase, falls substantially in vanadia-containing catalysts as a result of V^{4+} ions being incorporated into the support structure. The diffusion of vanadium ions into the anatase lattice causes the concentration of the vanadia-like surface species to decrease. Simultaneous worsening of the epitaxial relations between the vanadia-like monolayers and the support may cause some detachment of the active species and possibly their complete loss. The specific surface area of the alkoxy-derived Ti–Sn rutile support is comparable [4] with that of anatase used for commercial catalysts. According to Kumar et al. [5] tin addition is necessary to obtain rutile gel. Such rutile was used in this paper as a support for V-O-Mo catalyst, synthesis of which was performed by sol–gel method.

The purpose of this paper is to present V-O-Mo/Ti(Sn)O_2 catalyst obtained by sol–gel method from isopropoxide substrates. The morphology, phase composition and surface structure of the above catalyst are compared with the same physicochemical properties of the V-O-Mo/TiO_2 (anatase) catalyst with the same V:Mo:(Ti + Sn) ratio (1:9:90), obtained by the same method from inorganic substrates. The differences in the physicochemical properties of both catalysts are treated and discussed as having originated mainly from the differences in synthesis on hydrolysis and condensation level.

2. Experimental

2.1. Synthesis of the rutile-supported V-O-Mo catalyst

The precursor of a rutile-supported V-O-Mo catalyst with V:Mo:Ti:Sn = 1:9:72:18 was prepared by sol–gel method. The synthesis comprised two steps: obtainment of the rutile support and deposition of the V-O-Mo active phase on that support. The rutile support, with the addition of tin, was obtained from $Ti(OC_3H_7)_4$ (Aldrich) and $SnCl_4$ (Aldrich). The mixture of both compounds in isopropanol was added drop by drop to water

* Corresponding author.
E-mail address: kornelak@chemia.uj.edu.pl (P. Kornelak).

0920-5861/$ – see front matter © 2006 Elsevier B.V. All rights reserved.
doi:10.1016/j.cattod.2006.08.042

containing a small amount of isopropanol. Whole procedure is described in ref. [4]. To deposit a catalyst precursor on the support, hydrolysis of the molybdenyl and vanadyl isopropoxide mixture and next condensation of the hydroxocomplexes were performed in a $Ti(Sn)O_2$ sol solution. The $MoOCl_4$ (Aldrich) was dissolved in isopropanol (Mo:C_3H_7OH = 1:59) to obtain $MoO(OC_3H_7)_4$. $VO(OC_3H_7)_3$ (Aldrich) was added to this solution (V:Mo = 1:9). The mixture was heated to 353 K and kept at this temperature for 2 h under stirring. $Ti(Sn)O_2$ was suspended in water in the course of the 2 h stirring at 353 K. The 21.8 wt.% $Ti(Sn)O_2$ sol was added in one portion to the isopropanol solution (V:Mo:Ti:Sn = 1:9:72:18) and the mixture was kept at 353 K and stirred until evaporation was completed. The obtained xerogel was dried at 393 K for 7 days and calcinated in air at 733 K for 3 h.

2.2. Equipment used for physicochemical characterisation of the catalyst

Surface specific area and porosity were measured using an ASAP 2010 MICROMETRICS instrument. Before measurement the sample was outgassed at 378 K, for 36 h, in He atmosphere 10^{-3} Torr.

Phase identification and determination of crystallite size in the catalyst were performed using XRD patterns, Selected Area Diffraction (SAD) patterns and High Resolution Transmission Electron Microscopy (HRTEM) images. A Philips Analytical PW3710 X'PERT diffractometer with Cu Kα radiation was used for XRD measurements. The sampling width was 0.02 [°2Θ] and the scanning speed 0.02 [°2Θ/s].

A Philips CM 20 TEM equipped with an Energy Dispersive X-ray Spectrometer (EDXS) was applied to take selected area diffraction patterns and dark field (DF) images of the catalyst. The powdered samples were placed on a carbon film deposited on copper grids.

A Philips CM 200 FEG TEM was used to take high-resolution images. The specimens for TEM investigation were prepared by dispersing a small amount of powder samples in methanol and depositing them on the holey carbon film, supported on copper grid.

The surface composition was investigated using an ESCA 150 Spectrometer (VSW Scientific Instruments) with a magnesium anode as an X-ray source hemispherical analyser 150 mm in diameter and a Leybold multichannel detector. Sample was prepared for measurement by sticking them onto double-sided tape. The binding energy scale was established by referring to the C 1s value of the adventitious carbon (284.6 eV). In quantitative analysis of deconvoluted XPS bands, the following atomic sensitivity factors were used: Ti 2p = 1.8, Sn $3d_{5/2}$ = 4.3, Mo 3d = 2.75 and V 2p = 1.95 [6].

The structure of the surface species was determined by FT Raman spectroscopy.

A BIO-RAD FT Raman spectrometer with a Spectra Physics Nd:YAG Laser with an excitation line of 1064 nm was used. The sampling width was 2 cm^{-1}. The Raman spectrum in the wave number range of 80–1200 cm^{-1} is discussed.

2.3. The equipment used for catalytic tests

0.1 g of rutile-supported V-O-Mo catalyst was placed on a quartz wool in a quartz reactor with 4 mm internal diameter. The reaction mixture contained 100 ppm NO and 5 or 10 vol.% of O_2 and He as a balance. The GHSV value of the mixture was equal to 24,500 h^{-1}. A Stanford Research Systems QMS 100 Series Gas Analyzer was used as the detector. The catalyst was heated at 723 K in an oxygen stream for 1 h before the catalytical tests. These tests were carried out at four temperatures: 433, 503, 553 and 603 K. During the tests, the formation of N_2O and NO_2 was not observed.

3. Result and discussion

The specific BET surface area of the catalyst is equal to 69 m^2/g and the predominant pore radius is equal to 8.26 nm. This value of the specific surface area is comparable to the specific surface area of anatase-supported V-O-Mo catalysts (79–68 m^2/g) with vanadia loading in the range 0–1.5%, w/w investigated by Casagrande et al. [7].

An XRD pattern of the catalyst is shown in Fig. 1. The maxima of XRD fit to three phases: rutile [8], orthorhombic MoO_3 [9] and monoclinic β-MoO_3 [10,11]. Crystallite size of rutile in the [1 1 0] direction, calculated using Scherrer equation [12], is equal to 9.1 nm; for the o-MoO_3 (being the main Mo–O phase) in the [0 2 0] direction it is equal to 26 nm. Thus, the crystallites of o-MoO_3 are bigger than the rutile ones. The metastable β-MoO_3 phase could be created in the course of heating the catalyst precursor up to 623 K. Over 623 K, according to McCarron [11], this phase transforms to orthorhombic molybdena. It is thus evident that transformation during heating the catalyst precursor above 623 K was not completed. The lack of maxima which fit to vanadium oxides or mixed V-O-Mo phases shows that the nanocrystallites of these phases are absent or much smaller than for rutile and molybdena.

In Fig. 2, SAD pattern (a) and dark field image (b) taken with the use of the most intensive beam, of the rutile-supported V-O-Mo catalyst particle are presented. The $d_{h\,k\,l}$ values were calculated from the radii of the circles seen in SADP. All values match well to rutile lines. However, the first six reflections match to o-MoO_3 pattern as well. The average size of crystallites calculated from DF image is ca. 8 nm, which means that the rutile crystallites are the most numerous.

The other method used for phase identification and crystal size determination was HRTEM. The obtained results were expected to confirm the data from XRD and TEM and to give new information about minor phases in the system. One of 36 examined HRTEM images, being the most typical is shown in Fig. 3. The rutile nanocrystallite with the size 5.25 nm × 8.25 nm surrounded by amorphous xerogel is seen. Fourier transform of this nanocrystallite is presented in the left upper corner of the image.

In the summary of the phase identification in rutile-supported V-O-Mo catalyst, it can be claimed that the catalyst is composed mostly of rutile and o-MoO_3 crystallites.

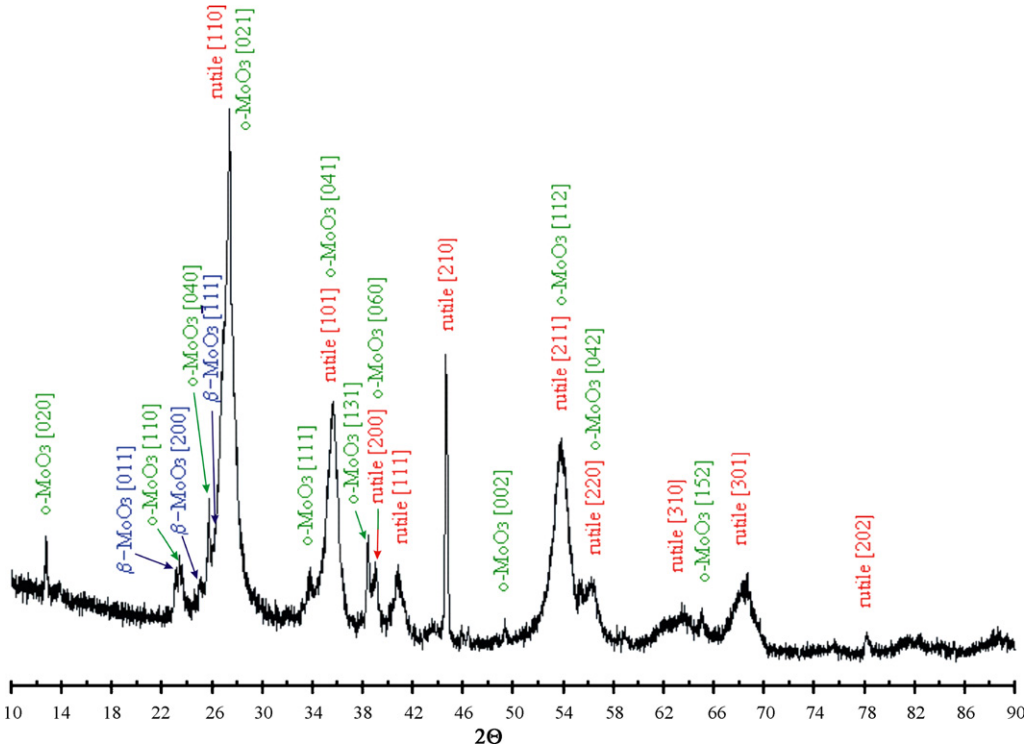

Fig. 1. XRD pattern of the rutile-supported V-O-Mo catalyst.

XPS measurements were performed to determine chemical composition of the catalyst surface nanolayers. The vanadium 2p band was deconvoluted to the peaks corresponding to V^{5+} (V_2O_5) $2p_{3/2}$ 517.5 eV, V^{4+} (V_2O_4) $2p_{3/2}$ 516.2 eV, V^{3+} (V_2O_3) $2p_{3/2}$ 515.3 eV and V^{2+} (VO) $2p_{3/2}$ 514.3 eV [13–15]. The results of the XPS quantitative analysis are presented in Table 1. The content of molybdenum is ca. two times higher and the content of vanadium is 2.4 times higher than assumed in synthesis. Thus, Mo occurs probably as surface species on rutile crystallites and form large crystallites of o-MoO_3. A dissolution of V in o-MoO_3 crystallites is rather poor [16] but the metastable β molybdena may have a higher capacity for V. It may be speculated that such a V_2O_5/MoO_3 solution with β-MoO_3 structure may first be formed in the course of the xerogel heating at a lower temperature and undergo segregation yielding V-O-Mo species on o-MoO_3 crystallites. It is also possible that V occurs together with Mo on rutile crystallites.

The structures of the surface species were studied with Raman spectroscopy. In Fig. 4, the FT Raman spectrum in the 80–1200 cm^{-1} range is shown. The broad peaks at 438 and 615 cm^{-1} are assigned to the rutile [17,18]. The narrower peaks at 127, 158, 245, 291, 338, 380, 665, 818, 849, 995 and 1136 cm^{-1} are ascribed to the orthorhombic molybdena [19–24]. The peak at position 970 cm^{-1} can be ascribed to

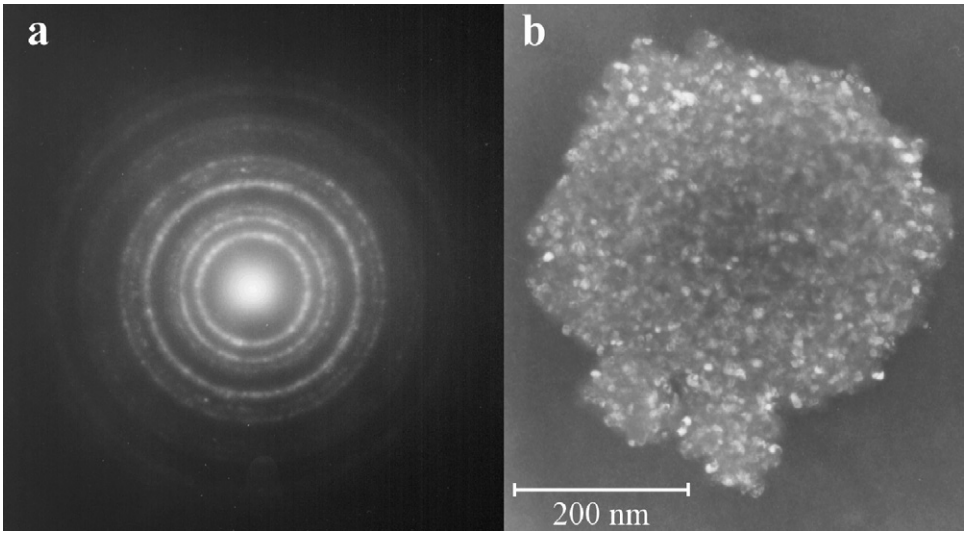

Fig. 2. (a) SAD pattern and (b) TEM dark field image (DF) of the rutile-supported V-O-Mo catalyst.

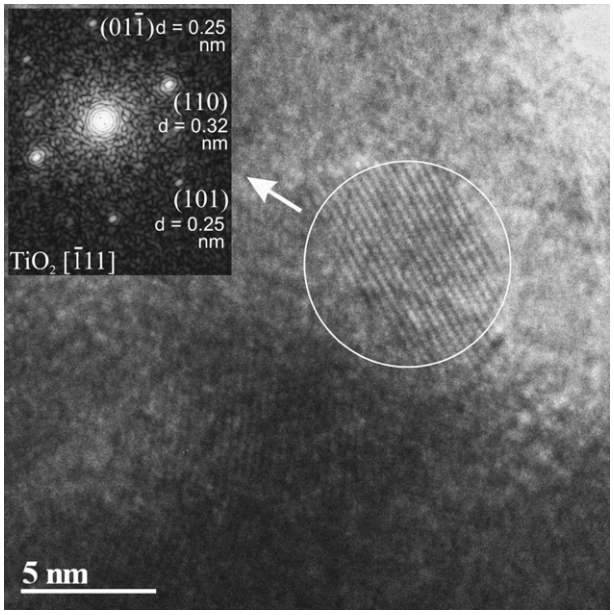

Fig. 3. HRTEM image of the rutile-supported V-O-Mo catalyst. The right part of the image reveals fringes corresponding to the TiO_2 shown in the [$\bar{1}$ 1 1] direction. The Fourier transform of this area is shown in the upper left corner.

monolayer forms of V_2O_5 and/or MoO_3 [24] and the shoulder at ca. 870 cm^{-1} to Mo=O in vanadia structure as was earlier observed and calculated for the V-O-W catalyst [25]. The presence of peaks at 528 and 698 cm^{-1} from bridging V–O bond vibrations in vanadia structure shows the presence of non-monomeric vanadia-like species. The presence of peaks from V–O bond vibration and the lack of V_2O_5 reflection in XRD pattern (Fig. 1) suggests that vanadia forms two-dimensional V-O-Mo species.

Table 1
XPS results for the V-O-Mo catalyst stored in ambient conditions

Element	BE [eV]	Content [at.%]
Ti	458.9	63.5
Sn	486.5	16.4
Mo	232.9	18.8
V^{5+}	517.5	0.2
V^{4+}	516.2	1.2
V^{3+}	515.3	0.1
V^{2+}	514.3	0.9

The physicochemical characterisation of rutile-supported V-O-Mo catalyst should be compared with those of anatase-supported V-O-Mo catalyst [2] to discuss the role of the support in catalyst structure formation. Both catalysts were synthesized using sol–gel method using the ratio V:Mo:Ti or Ti + Sn = 1:9:90. In the anatase-supported catalyst, anatase was the only phase detected by XRD and electron diffraction. In Raman spectrum, apart from the anatase peaks only peak at 970 cm^{-1} showing the presence of V_2O_5 were observed. The peak at ca. 970 cm^{-1} may also come from dispersed molybdena. According to Kornelak et al. [2], the catalyst consists of anatase nanocrystallites (~6.7 nm) with vanadia-like monolayer species and dispersed molybdenum oxide. The differences in phase content and the size of molybdenum oxide crystallities of both the V-O-Mo catalysts can be attributed to the differences in the nature of the supports. OH groups on the anatase are more basic than those on the rutile containing tin. Therefore, condensation of the hydroxocomplexes of molybdenum and of vanadyl occurs predominantly on the anatase surface. However, surface OH groups of rutile support esentially do not take part in the condensation process. The

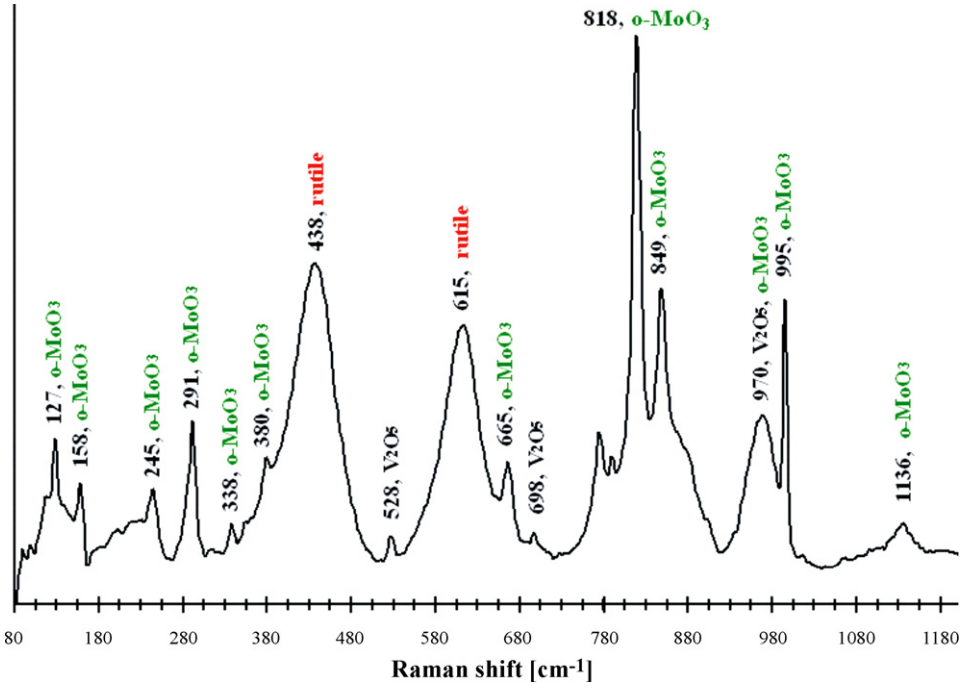

Fig. 4. FT Raman spectra, in the 80–1200 cm^{-1} range of rutile-supported V-O-Mo catalyst.

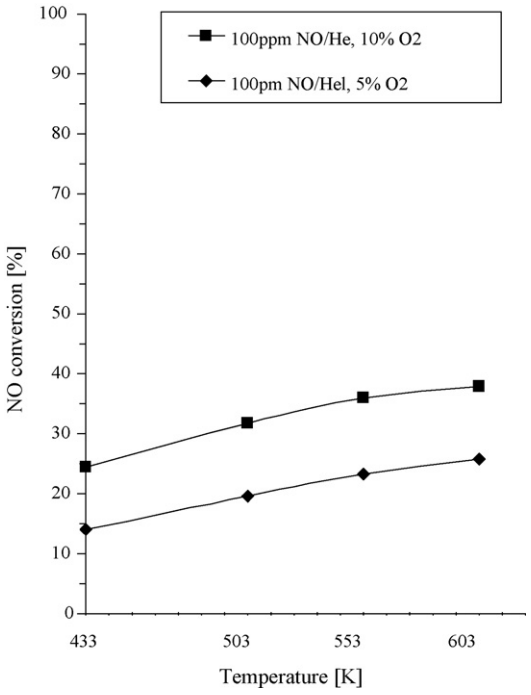

Fig. 5. NO conversion as a function of temperature on rutlie-supported V-O-Mo catalyst (100 ppm NO, 10 or 5 vol.% O_2, He as the balance, GHSV = 24,500 h^{-1}) over the catalyst heated at 723 K in an oxygen stream for 1 h.

same phenomenon was earlier observed during the synthesis of the rutile- and anatase-supported V-O-W catalysts [26].

NO conversion in the presence of 5 and 10 vol.% of oxygen are presented in Fig. 5. An increase of NO conversion with temperature for both feeds is observed. The catalyst activity in the feed is higher in the presence of 10 vol.% of O_2 than of 5 vol.% of O_2. As neither N_2O nor NO_2 was present in the products, the increase of the catalyst activity with the increase of the O_2 content in the feed should be ascribed to catalyst surface reconstruction caused by oxidation-induced surface vanadium segregation, as described elsewhere [27]. The heating of catalyst in oxidation atmosphere results in enrichment of surface nano-layers with vanadium and the formation of vanadia-like monolayer species. The higher amount of oxygen (10 vol.%) in the reaction mixture seems to better stabilize these species on catalyst surface than does the 5 vol.% of O_2.

4. Conclusions

Sol–gel method was used to synthesise a rutile-supported V-O-Mo catalyst with a specific BET surface area (69 m^2/g), comparable with that of anatase used in commercial V-O-Mo catalysts.

Rutile, orthorhombic molybdena and monoclinic β-MoO_3 phases were found by XRD and electron diffraction (SADP) in the catalyst. Given that molybdena crystallites are not formed in catalysts obtained by sol–gel method, one can conclude that V=O and Mo hydrocomplexes formed in the course of the sol–gel synthesis undergo condensation with anatase, but not with Ti(Sn) rutile surface.

Monolayer vanadia-like species containing some Mo atoms substituted for V ones are formed on molybdena crystallites. The observed catalyst activity in NO decomposition is thought to originate from these vanadia-like monolayer species.

Acknowledgement

This paper was partially supported by a grant from the Ministry of Education and Science (KBN) (Grant No. 4T09A 127 25).

References

[1] P. Kornelak, J. Banaś, A. Białas, M. Najbar, in: Proceedings of Jumelage—Matériaux Carbonés et Catalytiques pour L'Environnement, Zakopane, 3-8 X, (2002), p. 225.
[2] P. Kornelak, D.S. Su, C. Thomas, E. Bielańska, J. Camra, A. Wesełucha-Birczyńska, M. Najbar, Catal. Today, in preparation.
[3] L.E. Depero, J. Solid State Chem. 104 (1997) 470.
[4] M. Najbar, F. Mizukami, A. Białas, J. Camra, A. Wesełucha-Birczyńska, H. Izutsu, A. Góra, Top. Catal. 11/12 (2000) 13.
[5] K.P. Kumar, K. Keizer, A.J. Burggraaf, T. Okubo, H. Nagamoto, J. Mater. Chem. 3 (1993) 923.
[6] D. Briggs, M.P. Seah (Eds.), second ed., Practical Surface Analysis: Auger and X-ray Photoelectron Spectroscopy, vol. 1, John Wiley & Sons Ltd., 1990, pp. 636–637.
[7] L. Casagrande, L. Lietti, I. Nova, P. Forzatti, A. Baiker, Appl. Catal. B 22 (1999) 63.
[8] National Bureau of Standards, Monogr., Sec. 7, 1969, 25, ASTM Card 21-1276.
[9] National Bureau of Standards, Monogr., 25 (20), 1984, 118, ASTM Card 35-0609.
[10] ASTM Card 37-1445.
[11] E.M. McCarron, J. Chem. Soc., Chem. Commun. 4 (1986) 336.
[12] H. Klug, L. Alexander, X-Ray Diffraction Procedures, Wiley, New York, 1974, p. 687.
[13] C.D. Wagner, A.V. Naumkin, A. Kraut-Vass, J.W. Allison, C.J. Powell, J.R. Rumble Jr., NIST X-ray Photoelectron Spectroscopy Database, NIST Standard Reference Database 20, Version 3.4 (Web Version), Distributed by the Measurement Services Division of the National Institute of Standards and Technology (NIST) Technology Services, http://srdata.nist.gov/xps/.
[14] R. Benoit, CNRS Orléans, http://www.lasurface.com.
[15] C.D. Wagner, W.M. Riggs, L.E. Davis, J.F. Moulder, G.E. Mullenberg (Eds.), Handbook of X-ray Photoelectron Spectroscopy, Perkin-Elmer Corporation, Physical Electronics Division, 1978.
[16] K. Khulbe, R. Mann, A. Manoogien, J. Chem. Phys. 60 (1974) 480.
[17] A. Białas, E. Bielańska, B. Borzęcka-Prokop, H. Hobert, J. Camra, M. Najbar, J. Sonnefeld, W. Vogelsberger, Pol. J. Environ. Stud. 10 (II) (2001) 36.
[18] U. Balachandran, N.G. Eror, J. Solid State Chem. 42 (1982) 276.
[19] V. Belokopytov, K. Kholyavenko, S. Gerei, J. Catal. 60 (1979) 1.
[20] K.V.R. Chary, V.V. Rao, G. Muralidhar, P.K. Rao, Catal. Lett. 7 (1990) 389.
[21] A.N. Desikan, L. Huang, S.T. Oyama, J. Chem. Soc., Faraday Trans. 88 (22) (1992) 3357.
[22] L. Seguin, M. Figlarz, R. Cavagnat, J.-C. Lassègues, Spectrochim. Acta A 51 (1995) 1323.
[23] H. Hu, I.E. Wachs, S.R. Bare, J. Phys. Chem. 99 (1995) 10897.
[24] H. Knözinger, Catal. Today 32 (1996) 71.
[25] M. Najbar, E. Brocławik, A. Góra, J. Camra, A. Białas, A. Wesełucha-Birczyńska, Chem. Phys. Lett. 325 (2000) 330.
[26] M. Najbar, F. Mizukami, H. Izutsu, Pol. J. Environ. Stud. 9 (I) (2000) 45.
[27] P. Kornelak, F. Mizukami, A. Wesełucha-Birczyńska, L. Proniewicz, G. Djega-Mariadassou, A. Białas, M. Najbar, Catal. Today 90 (2004) 103.